



Article

Sol–Gel Synthesis and Characterization of Coatings of Mg–Al Layered Double Hydroxides

A. Smalenskaite ¹, M. M. Kaba ², I. Grigoraviciute-Puroniene ¹, L. Mikoliunaite ^{1,3}, A. Zarkov ¹ , R. Ramanauskas ³, I. A. Morkan ² and A. Kareiva ^{1,*} 

¹ Department of Inorganic Chemistry, Faculty of Chemistry, Vilnius University, Vilnius LT-03225, Lithuania; aurelija.smalenskaite@gmail.com (A.S.); inga.grigoraviciute@gmail.com (I.G.-P.); lina.mikoliunaite@chf.vu.lt (L.M.); aleksej.zarkov@chf.vu.lt (A.Z.)

² Department of Chemistry, Institute of Natural Sciences, Bolu Abant Izzet Baysal University, 14030 Bolu, Turkey; musakaba136@yahoo.com (M.M.K.); morkan_i@ibu.edu.tr (I.A.M.)

³ Center for Physical Sciences and Technology, LT-10257 Vilnius, Lithuania; rimantas.ramanauskas@ftmc.lt

* Correspondence: aivaras.kareiva@chgf.vu.lt; Tel.: +37061567428

Received: 29 October 2019; Accepted: 11 November 2019; Published: 13 November 2019



Abstract: In this study, new synthetic approaches for the preparation of thin films of Mg–Al layered double hydroxides (LDHs) have been developed. The LDHs were fabricated by reconstruction of mixed-metal oxides (MMOs) in deionized water. The MMOs were obtained by calcination of the precursor gels. Thin films of sol–gel-derived Mg–Al LDHs were deposited on silicon and stainless-steel substrates using the dip-coating technique by a single dipping process, and the deposited film was dried before the new layer was added. Each layer in the preparation of the Mg–Al LDH multilayers was separately annealed at 70 °C or 300 °C in air. Fabricated Mg–Al LDH coatings were characterized by X-ray diffraction (XRD) analysis, scanning electron microscopy (SEM), and atomic force microscopy (AFM). It was discovered that the diffraction lines of Mg₃Al LDH thin films are sharper and more intensive in the sample obtained on the silicon substrate, confirming a higher crystallinity of synthesized Mg₃Al LDH. However, in both cases the single-phase crystalline Mg–Al LDHs have formed. To enhance the sol–gel processing, the viscosity of the precursor gel was increased by adding polyvinyl alcohol (PVA) solution. The LDH coatings could be used to protect different substrates from corrosion, as catalyst supports, and as drug-delivery systems in medicine.

Keywords: layered double hydroxides; Mg–Al; sol–gel synthesis; coatings; spin coating; silicon; stainless steel

1. Introduction

Layered double hydroxides (LDHs) are compounds composed of positively charged brucite-like layers, with an interlayer gallery containing charge-compensating anions and water molecules. The metal cations occupy the centres of shared oxygen octahedra whose vertices contain hydroxide ions that connect to form infinite two-dimensional sheets [1–6]. A chemical formula of Mg–Al LDH can be expressed as $[\text{Mg}^{2+}_{1-x}\text{Al}^{3+}_x(\text{OH})_2]^{x+}(\text{A}^{m-})_{x/m}\cdot n\text{H}_2\text{O}$, where A^{m-} is an intercalated anion.

LDHs are widely used in commercial products as adsorbents, catalysts, flame retardants, osmosis membranes, energy-storage materials, and sensors [3,7–13]. LDH materials have been successfully used for drug and gene delivery, cosmetics, cancer therapy, biosensing, and as antibacterial agents [14–19]. LDHs have been studied for their potential application to the removal of anions and also toxic metal ions from contaminated waters [20–26]. In recent years, inorganic–organic hybrid luminescence materials have been widely investigated due to their novel properties of forming stable compounds with lanthanides in the interlayer space of LDHs [4,6,27–29]. The LDH layers were demonstrated to offer anticorrosion protection [30–34].

There are many general methods for the preparation of bulk LDHs, such as co-precipitation [2,35,36], sol-gel synthesis [4,5,37,38], urea hydrolysis [39,40], hydrothermal synthesis [41], and others [38,42,43]. Several synthesis methods were suggested for the fabrication of LDH coatings on different substrates. In [44–47], facile in situ growth and dispersing methods were used to prepare anticorrosive LDH films on the surfaces of different Al and Mg alloys. The LDH-sealing layers and coatings on anodic aluminium oxide, titanium dioxide, aluminium, steel alloys, and other metal substrates were also prepared using aqueous solution, hydrothermal, co-precipitation, or hybrid hydrothermal-co-precipitation methods [48–55]. Wu et al. [56] suggested the use of a urea hydrolysis method for the synthesis of LDH films on Al alloy. The urea-assisted synthetic approach was transferred for the fabrication of LDH coatings on a plasma electrolysis (PE) Al alloy coating [57]. Recently, formation processes for LDH coatings on Mg alloy or on alumina by the CO₂ pressurization and electrophoretic deposition methods, respectively, have been developed [58,59].

It is well-known that the sol-gel processing route for the preparation of thin films of different materials is a low-cost and simple method, which allows for better chemical homogeneity due to molecular-level mixing of the precursors [60–65]. However, the fabrication of LDH films by the sol-gel chemistry method has not been given sufficient attention to date. The number of such studies is rather limited, with only one publication [66]. Moreover, the authors of this study provided only the results about the preparation of amorphous Mg–Al–Eu–O thin films on silica glass substrates by a sol-gel dip-coating method with a heat treatment at 700 °C. Thus, no evidence of the formation of LDHs during sol-gel processing was documented and characterized. Therefore, the present study will discuss for the first time the stabilization of LDH films grown using a sol-gel synthetic approach on silicon and stainless-steel substrates by the dip-coating technique. The LDHs were fabricated by reconstruction of mixed-metal oxides (MMOs) in deionized water. The MMOs were obtained by calcination of the precursor gels.

2. Experimental

The Mg₃Al LDH specimens were prepared by the sol-gel technique using metal nitrates Mg(NO₃)₂·6H₂O (99.9%, Fluka, Saint Louis, MO, USA) and Al(NO₃)₃·9H₂O (99.9%, Fluka, Saint Louis, MO, USA) dissolved in 50 mL of deionized water as starting materials. To the obtained mixture, a 0.2 M solution of citric acid (C₆H₈O₇, 99.0%, Alfa Aesar, Haverhill, MA, USA) was added. The resulting solution was additionally stirred for 1 h at 80 °C. Finally, 2 mL of ethylene glycol (C₂H₆O₂, 99.0%, Alfa Aesar, Haverhill, MA, USA) was added with continued stirring at 150 °C. During the evaporation of solvent, the transformations from the sols to the gels occurred. The synthesized precursor gels were dried at 105 °C for 24 h. The MMOs were obtained by heating the gels at 650 °C for 4 h. LDHs were fabricated by reconstruction of MMOs in deionized water at 80 °C for 6 h. The relative humidity of the atmosphere was about 50%. Mg₃Al LDH coatings were synthesized using the sol-gel method in different solutions. In the first attempt, only an aqueous solution of LDH was used. Secondly, 0.5 g of LDH was mixed with 1 g of polyvinyl alcohol (PVA) (PVA7200, 99.5%, Aldrich, Saint Louis, MO, USA) in distilled water. LDH suspensions were deposited on silicon and stainless-steel substrates using the dip-coating technique by a single dipping process, and the deposited film was dried before the new layer was added.

X-ray diffraction (XRD) analysis of synthesized compounds was performed with a MiniFlex II diffractometer (Rigaku, The Woodlands, TX, USA) using primary-beam Cu K α radiation ($\lambda = 1.541838$ Å). The 2 θ ° angle of the diffractometer was tuned from 8 to 80° in steps of 0.02°, with the measuring time of 0.4 s per step. The surface morphological features were characterized using a scanning electron microscope (SEM) (Hitachi SU-70, Tokyo, Japan). The roughness of the Mg₃Al LDH films was estimated using an atomic force microscope (AFM) (BioscopeII/Catalyst, Karlsruhe, Germany). The ScanAsyst, operated in the peak-force tapping mode and equipped with a wafer of silicon nitride probe Asyst at the air AFM tip, was used for imaging. Surface root mean square (RMS) values were calculated using the MATLAB R2015b programme.

3. Results and Discussion

The XRD patterns of Mg_3Al LDHs obtained from the silicon and steel substrates are presented in Figures 1 and 2, respectively. Evidently, the intensity of Si reflection originating from the substrate is much higher in comparison to the main reflection of LDH samples. However, after eliminating silicon reflection from the XRD patterns (see the insertion in Figure 1), the main reflections clearly represent the formation of an LDH structure after 15 dipping procedures. The formation of Mg_3Al LDH thin films on stainless-steel substrate (Figure 2) was also observed. The diffraction lines of Mg_3Al LDH thin films are sharper and more intense for the sample obtained from the silicon, confirming higher crystallinity of synthesized Mg_3Al LDH. In both cases, the single-phase crystalline LDHs have formed [4–6].

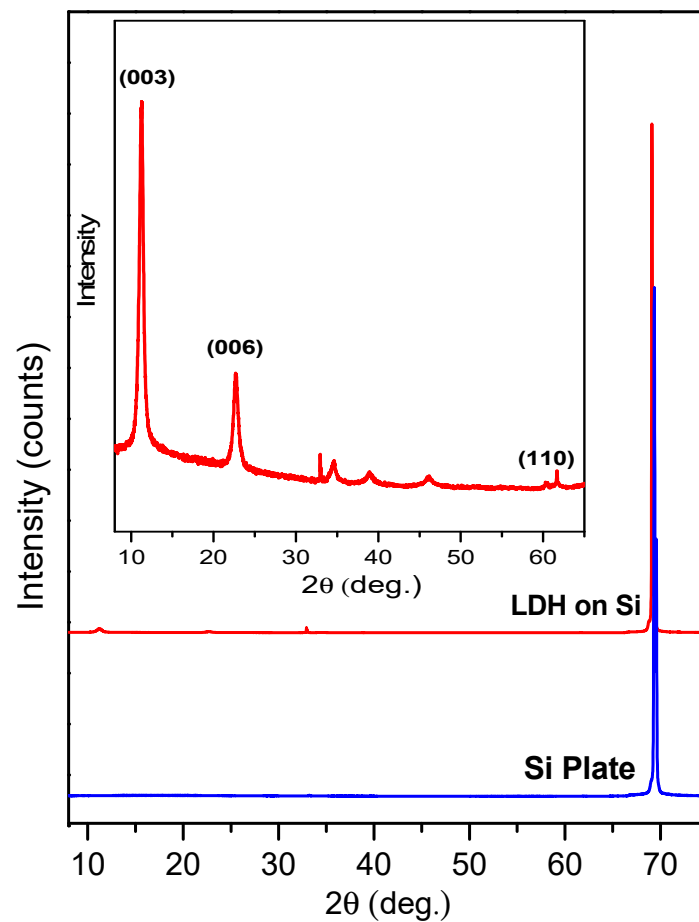


Figure 1. X-ray diffraction (XRD) pattern of the Mg_3Al layered double hydroxide (LDH) coating on silicon substrate, using 15 layers of precursor at 70 °C.

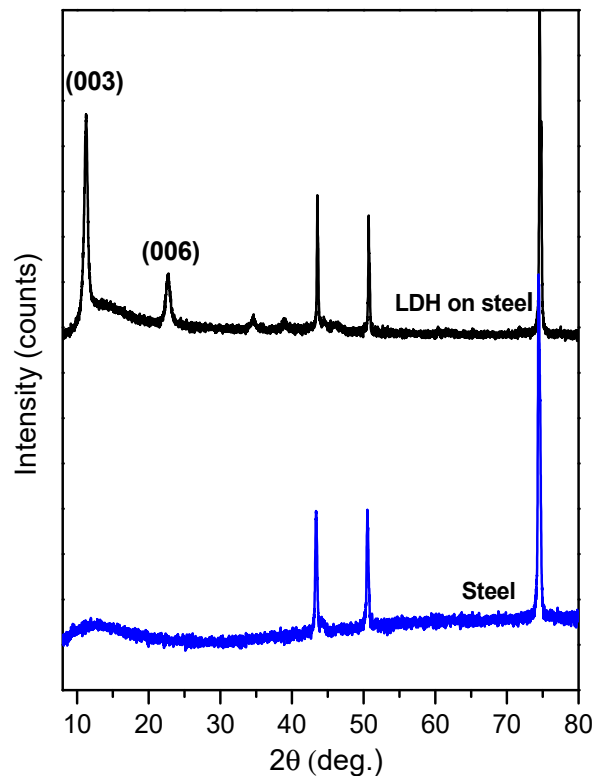


Figure 2. XRD pattern of the Mg_3Al LDH coating on stainless-steel substrate, using 15 layers of precursor at 70 °C.

The surface morphology of the representative Mg_3Al LDH film sample obtained from the Si substrate is presented in Figure 3. The surface of the substrate is covered with a monolithic layer of agglomerated plate-like particles that are 5–10 μm in size. However, the SEM micrographs obtained at a higher magnification clearly show that these plate-like particles are composed of hexagonally shaped nanoparticles that are characteristic of LDH structures [6]. An almost identical surface morphology was observed for the LDH coatings on the stainless-steel substrate.

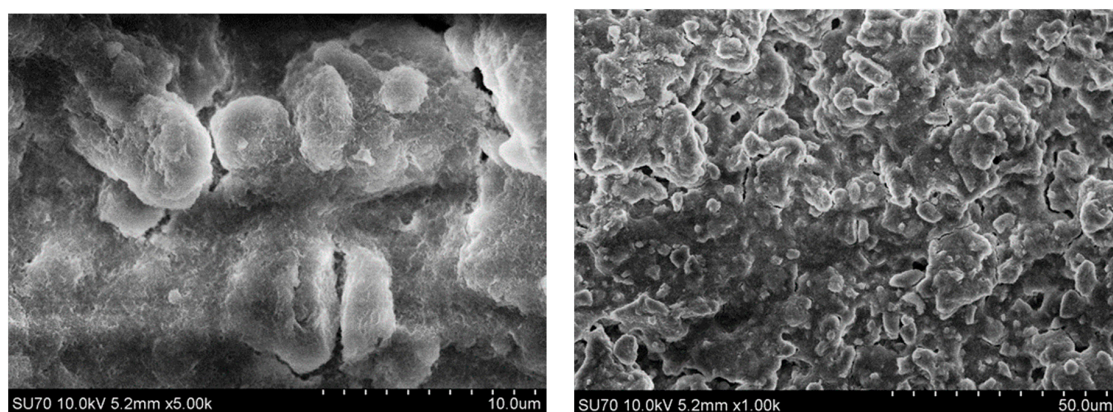


Figure 3. Scanning electron microscopy (SEM) micrographs of Mg_3Al LDH film on silicon substrate, obtained at different magnifications.

The sol–gel synthesis processing route for high-quality calcium hydroxyapatite coatings on silicon substrate when PVA was used as a gel-network-forming agent [67] was a source of inspiration for this study. Therefore, to enhance the sol–gel processing, the viscosity of the precursor gel was increased by adding PVA solution, and the drying temperature was also increased.

The XRD patterns of the LDH coatings obtained from Si (Figure 4) and stainless-steel (Figure 5) substrates, however, were almost the same as without the addition of PVA.

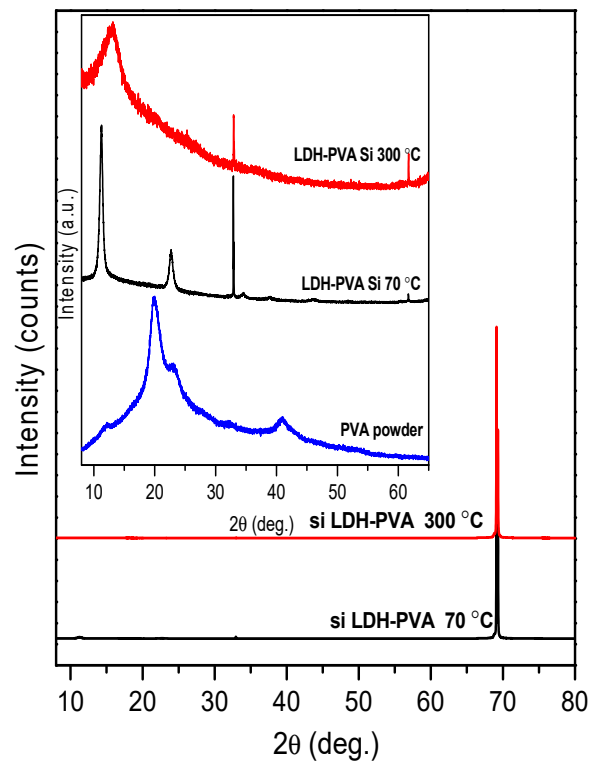


Figure 4. XRD patterns of the Mg_3Al LDH coatings on silicon substrate using 15 layers of precursor with PVA solution, obtained at 70 °C and 300 °C.

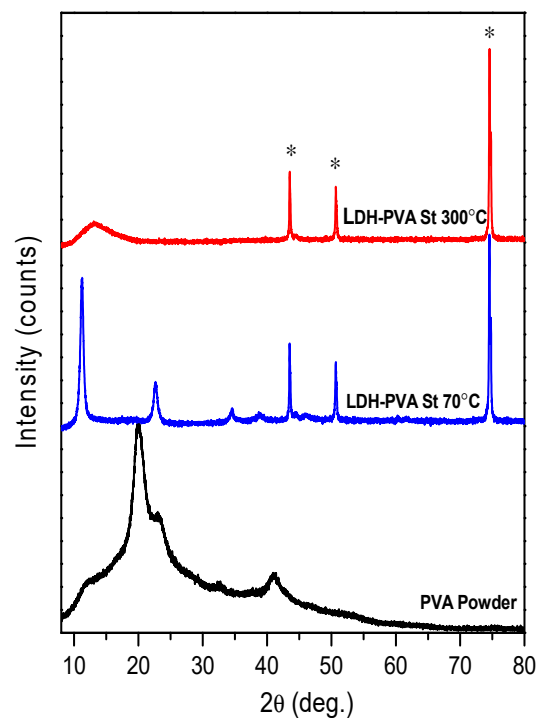


Figure 5. XRD patterns of the Mg_3Al LDH coatings on stainless-steel substrate using 15 layers of precursor in PVA solution, obtained at 70 °C and 300 °C. Reflections of stainless steel are marked: *.

The XRD patterns show the formation of the same crystallinity LDH phase on the Si substrate. With the dip-coating in PVA solution and drying at 300 °C (PVA's melting point is ~266 °C), the LDH phase did not form. The LDH sample with higher crystallinity was obtained from the steel substrate. Interestingly, no side iron oxide (Fe_2O_3 and Fe_3O_4) phases were formed during the synthesis, as was observed in the case of sol-gel synthesis of calcium hydroxyapatite on stainless-steel substrate [63].

The SEM micrographs of Mg_3Al LDH films obtained from Si and stainless-steel substrates using a precursor in the PVA solution are shown in Figure 6. The formation of nanograins of LDH is evident when PVA solution was used in the sol-gel processing. Moreover, these nanograins show a tendency to form cloudy agglomerates.

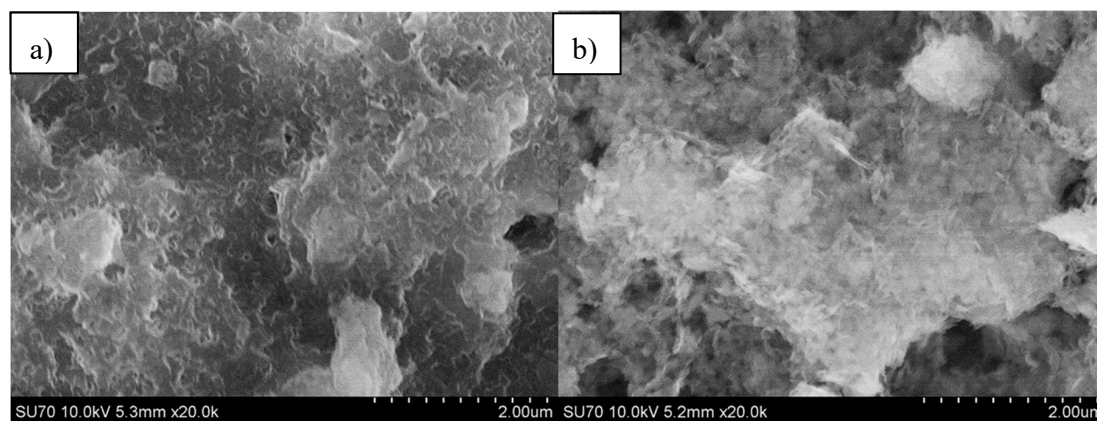


Figure 6. SEM micrographs of Mg_3Al LDH films obtained on silicon (a) and stainless-steel (b) substrates in PVA solution at 70 °C.

The amount of water, hydroxide, and carbonate in the formula of synthesized bulk LDH samples can be calculated from the results of thermogravimetric analyses [6,68]. For example, the composition was defined in our previous study to be $[\text{Mg}_{0.75}\text{Al}_{0.25}(\text{OH})_2](\text{CO}_3)_{0.125}\cdot 4\text{H}_2\text{O}$ [6]. However, the experimental procedure could be more complicated in the case of thin films and should be redefined in the future.

In Figures 7–10, atomic force microscopy images of different Mg_3Al LDH films prepared before and after modification on silicon and stainless-steel substrates are represented. The atomic force microscopy (AFM) data of LDH profiles were filtered with a mathematical procedure implemented in the MATLAB software. This software computes several roughness parameters at different “walks” of axes x (vertical) and y (horizontal) positions (see Table 1). For this reason, the AFM images were reduced and cut off from the middle $10\ \mu\text{m}^2$ square for a better comparison. Figures 7 and 8 show the Mg_3Al LDH films dip-coated on the silicon and stainless-steel substrates, respectively.

Table 1. The calculated root mean square (RMS) parameters from AFM images of Mg_3Al LDH coatings, with standard deviations in parentheses.

Sample	Average RMS X (nm)	Average RMS Y (nm)	Average RMS (nm)	Min Height (nm)	Max Height (nm)	Average Heights (nm)
LDH film on silicon	172.78(8)	170.99(6)	186.14(8)	−500	500	−43.48(5)
LDH film on stainless steel	334.26(7)	345.86(7)	352.62(9)	−1000	1000	−67.55(5)
LDH film on silicon with PVA	398.66(9)	691.39(7)	733.30(8)	−2000	2000	135.03(6)
LDH film on stainless steel with PVA	774.36(8)	778.69(9)	1181.12(7)	−2000	2000	−858.89(5)

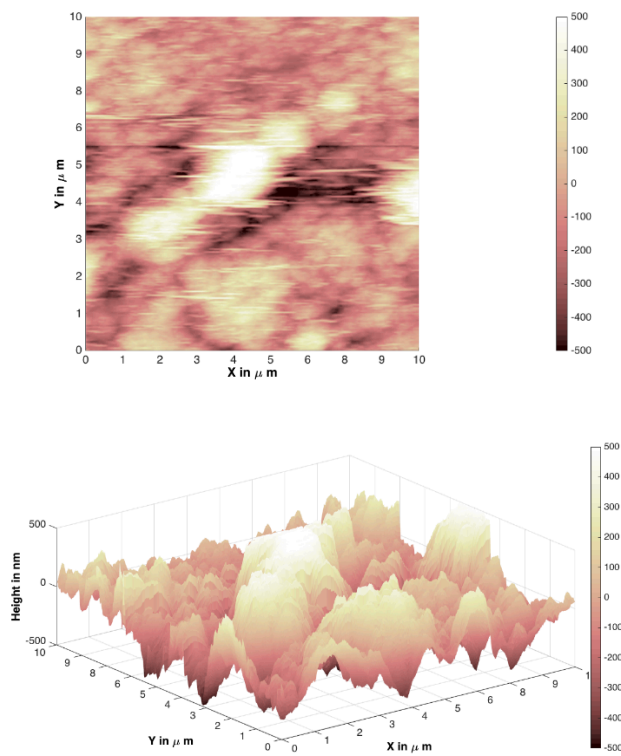


Figure 7. Atomic force microscopy (AFM) images of a Mg_3Al LDH film on silicon substrate at $70\text{ }^\circ\text{C}$.

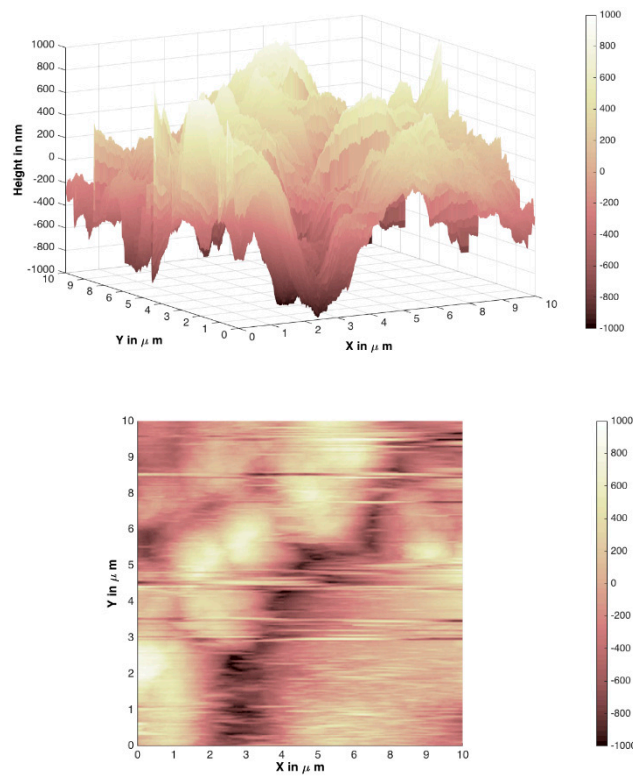


Figure 8. AFM images of a Mg_3Al LDH film on stainless-steel substrate at $70\text{ }^\circ\text{C}$.

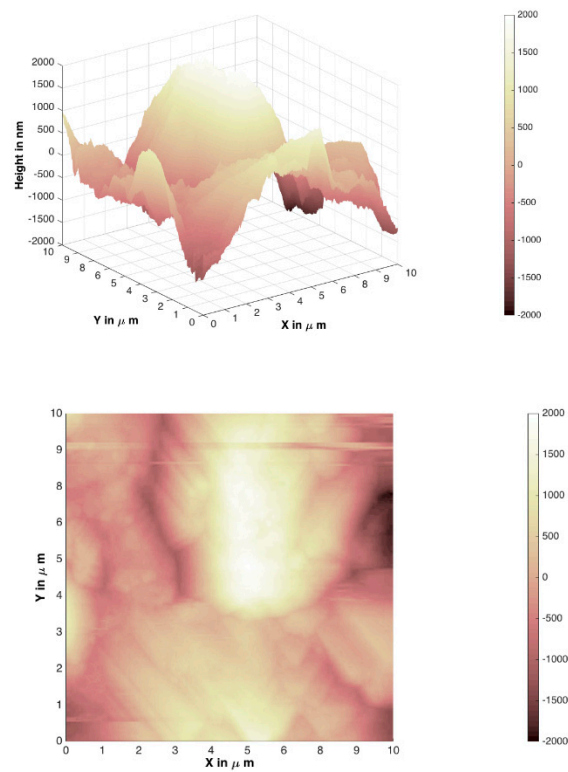


Figure 9. AFM images of the Mg_3Al LDH on silicon substrate in PVA solution at $70\text{ }^\circ\text{C}$.

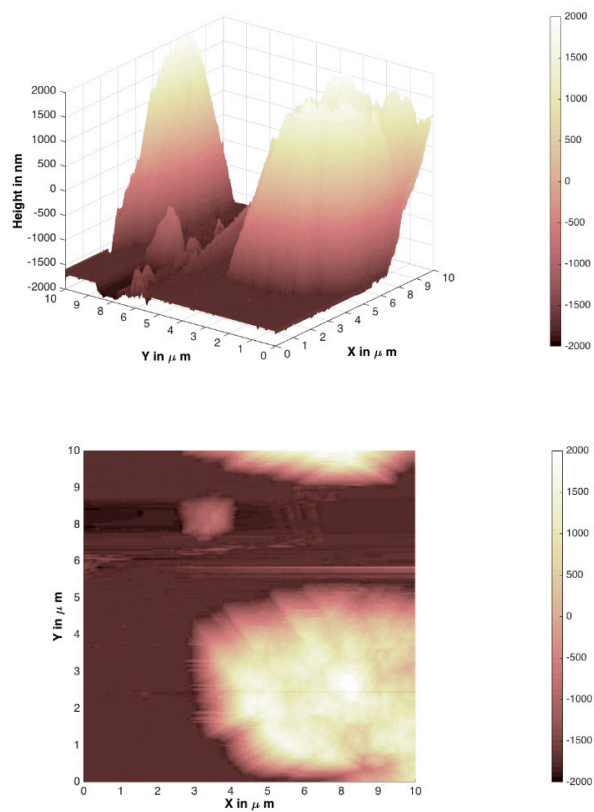


Figure 10. AFM images of the Mg_3Al LDH on stainless-steel substrate in PVA solution at $70\text{ }^\circ\text{C}$.

The average RMS parameter obtained by AFM was determined to be $186.14(8)$ nm for the Mg_3Al LDH surface on the silicon substrate ($64.89(7)$ nm for raw Si substrate) and $352.62(9)$ nm for the Mg_3Al

LDH surface on the stainless-steel substrate (112.54(8) nm for raw Fe substrate). However, using the PVA (Figures 9 and 10) solution for the modification of the Mg₃Al LDH synthesis, the roughness increased to 733.30(8) and 1181.12(7) nm on the silicon and stainless-steel substrates, respectively. This might be because the higher concentration of polymers resulted in the formation of larger micelles of the monomer in the solution and larger polymer aggregates on the surface. As we can see from the AFM images and the calculated RMS values, the synthesized LDH coatings can be characterized as nanometer-size thin films. It was observed that the Mg₃Al LDH film that formed on silicon substrate in the distilled water had the smoothest surface. The synthesized coatings could be applied for future work for the investigation of anticorrosive properties.

4. Conclusions

Mg₃Al LDH coatings were successfully fabricated on silicon and stainless-steel substrates using the sol-gel processing route for the first time, to the best of our knowledge. The LDHs were fabricated by reconstruction of MMOs in deionized water. The MMOs were obtained by calcination of the precursor gels. The XRD patterns demonstrated the high crystallinity of the synthesized Mg₃Al₁ LDH coatings. The SEM micrographs clearly showed that the plate-like particles that formed on the surface are composed of hexagonally shaped nanoparticles, which are characteristic of LDH structures. The average RMS parameter obtained by AFM was determined to be 186.14(8) nm for the Mg₃Al LDH surface on the silicon substrate and 352.62(9) nm for the Mg₃Al LDH surface on the stainless-steel substrate. The roughness of the coatings increased to 733.30(8) and 1181.12(7) nm on the silicon and stainless-steel substrates, respectively, using the PVA solution for the modification of the Mg₃Al LDH. The phase purity of coatings obtained from Si and stainless-steel substrates, however, was almost the same with or without the addition of PVA.

Author Contributions: Formal Analysis, A.S., A.Z., R.R., and A.K.; Investigation, A.S., M.M.K., I.G.-P., A.Z., and L.M.; Resources, R.R., I.A.M., and A.K.; Data Curation, A.S.; Writing—Original Draft Preparation, A.S. and A.K.; Writing—Review and Editing, A.K.; Visualization, A.S. and M.M.K.; Supervision, I.A.M. and A.K.

Funding: This work was supported by a research grant (NOCAMAT, No. S-LB-19-2) from the Research Council of Lithuania.

Conflicts of Interest: The authors declare no conflicts of interest.

References

1. Rives, V. *Layered Double Hydroxides: Present and Future*; Nova Science Publishers: New York, NY, USA, 2001.
2. Salak, A.N.; Tedim, J.; Kuznetsova, A.I.; Ribeiro, J.L.; Vieira, L.G.; Zheludkevich, M.L.; Ferreira, M.G.S. Comparative X-ray diffraction and infrared spectroscopy study of Zn-Al layered double hydroxides: Vanadate vs nitrate. *Chem. Phys.* **2012**, *397*, 102–108. [[CrossRef](#)]
3. Serdechnova, M.; Salak, A.N.; Barbosa, F.S.; Vieira, D.E.L.; Tedim, J.; Zheludkevich, M.L.; Ferreira, M.G.S. Interlayer intercalation and arrangement of 2-mercaptobenzothiazolate and 1,2,3-benzotriazololate anions in layered double hydroxides: In situ X-ray diffraction study. *J. Solid State Chem.* **2016**, *233*, 158–165. [[CrossRef](#)]
4. Smalenskaite, A.; Vieira, D.E.L.; Salak, A.N.; Ferreira, M.G.S.; Katelnikovas, A.; Kareiva, A. A comparative study of co-precipitation and sol-gel synthetic approaches to fabricate cerium-substituted Mg-Al layered double hydroxides with luminescence properties. *Appl. Clay Sci.* **2017**, *143*, 175–183. [[CrossRef](#)]
5. Sokol, D.; Salak, A.N.; Ferreira, M.G.S.; Beganskiene, A.; Kareiva, A. Bi-substituted Mg₃Al-CO₃ layered double hydroxides. *J. Sol-Gel Sci. Technol.* **2018**, *85*, 221–230. [[CrossRef](#)]
6. Smalenskaite, A.; Pavasaryte, L.; Yang, T.C.K.; Kareiva, A. Undoped and Eu³⁺ doped magnesium-aluminium layered double hydroxides: Peculiarities of intercalation of organic anions and investigation of luminescence properties. *Materials* **2019**, *12*, 736. [[CrossRef](#)]
7. Zazoua, H.; Saadi, A.; Bachari, K.; Halliche, D.; Rabia, C. Synthesis and characterization of Mg-M (M: Al, Fe, Cr) layered double hydroxides and their application in the hydrogenation of benzaldehyde. *Res. Chem. Intermed.* **2014**, *40*, 931–946. [[CrossRef](#)]

8. Klemkaite-Ramanauskė, K.; Zilinskas, A.; Taraskevicius, R.; Khinsky, A.; Kareiva, A. Preparation of Mg/Al layered double hydroxide (LDH) with structurally embedded molybdate ions and application as a catalyst for the synthesis of 2-adamantylidene(phenyl)amine Schiff base. *Polyhedron* **2014**, *68*, 340–345. [[CrossRef](#)]
9. Hosni, K.; Abdelkarim, O.; Frini-Srasra, N.; Srasra, E. Synthesis, structure and photocatalytic activity of calcined Mg-Al-Ti-layered double hydroxides. *Korean J. Chem. Eng.* **2015**, *32*, 104–112. [[CrossRef](#)]
10. Li, H.J.; Su, X.Y.; Bai, C.H.; Xu, Y.Q.; Pei, Z.C.; Sun, S.G. Detection of carbon dioxide with a novel HPTS/NiFe-LDH nanocomposite. *Sens. Actuators B Chem.* **2016**, *225*, 109–114. [[CrossRef](#)]
11. Lu, P.; Liang, S.; Qiu, L.; Gao, Y.S.; Wang, Q. Thin film nanocomposite forward osmosis membranes based on layered double hydroxide nanoparticles blended substrates. *J. Membr. Sci.* **2016**, *504*, 196–205. [[CrossRef](#)]
12. Gao, M.X.; Zhang, M.H.; Li, Y.H. Investigation into 1,3-butadiene and other bulk chemicals' formation from bioethanol over Mg-Al catalysts. *RSC Adv.* **2017**, *7*, 11929–11937. [[CrossRef](#)]
13. Hashemi, A.B.; Kasiri, G.; Glenneberg, J.; Langer, F.; Kun, R.; La Mantia, F. Electrochemical and morphological characterization of Zn-Al-Cu layered double hydroxides as a negative electrode in aqueous zinc-ion batteries. *ChemElectrochem* **2018**, *5*, 2073–2079. [[CrossRef](#)]
14. Allou, N.B.; Saikia, P.; Borah, A.; Goswamee, R.L. Hybrid nanocomposites of layered double hydroxides: An update of their biological applications and future prospects. *Colloid Polym. Sci.* **2017**, *295*, 725–747. [[CrossRef](#)]
15. Cunha, V.R.R.; de Souza, R.B.; Martins, A.M.C.R.P.D.F.; Koh, I.H.J.; Constantino, V.R.L. Accessing the biocompatibility of layered double hydroxide by intramuscular implantation: Histological and microcirculation evaluation. *Sci. Rep.* **2016**, *6*, 30547. [[CrossRef](#)] [[PubMed](#)]
16. Hu, H.; Xiu, K.M.; Xu, S.L.; Yang, W.T.; Xu, F.J. Functionalized layered double hydroxide nanoparticles conjugated with disulfide-linked polycation brushes for advanced gene delivery. *Bioconjug. Chem.* **2013**, *24*, 968–978. [[CrossRef](#)] [[PubMed](#)]
17. Cao, Z.B.; Adnan, N.N.M.; Wang, G.Y.; Rawal, A.; Shi, B.Y.; Liu, R.Z.; Liang, K.; Zhao, L.Y.; Gooding, J.J.; Boyer, C.; et al. Enhanced colloidal stability and protein resistance of layered double hydroxide nanoparticles with phosphonic acid-terminated PEG coating for drug delivery. *J. Colloid Interface Sci.* **2018**, *521*, 242–251. [[CrossRef](#)] [[PubMed](#)]
18. Zhang, K.; Xu, Z.P.; Lu, J.; Tang, Z.Y.; Zhao, H.J.; Good, D.A.; Wei, M.Q. Potential for layered double hydroxides-based innovative drug delivery systems. *Int. J. Mol. Sci.* **2014**, *15*, 7409–7428. [[CrossRef](#)]
19. Yasaei, M.; Khakbiz, M.; Zamanian, A.; Ghasemi, E. Synthesis and characterization of Zn/Al-LDH@SiO₂ nanohybrid: Intercalation and release behaviour of vitamin C. *Mater. Sci. Eng. C Mater. Biol. Appl.* **2019**, *103*, 109816. [[CrossRef](#)]
20. Tezuka, S.; Chitrakar, R.; Sonoda, A.; Ooi, K.; Tomida, T. Studies on selective adsorbents for oxo-anions. Nitrate ion-exchange properties of layered double hydroxides with different metal atoms. *Green Chem.* **2004**, *6*, 104–109. [[CrossRef](#)]
21. Lazaridis, N.K.; Pandi, T.A.; Matis, K.A. Chromium(VI) removal from aqueous solutions by Mg-Al-CO₃ hydrotalcite: Sorption-desorption kinetic and equilibrium studies. *Ind. Eng. Chem.* **2004**, *43*, 2209–2215. [[CrossRef](#)]
22. Gillman, G.P. A simple technology for arsenic removal from drinking water using hydrotalcite. *Sci. Total Environ.* **2006**, *336*, 926–931. [[CrossRef](#)] [[PubMed](#)]
23. Frost, R.L.; Musumeci, A.W. Nitrate absorption through hydrotalcite reformation. *J. Colloid Interface Sci.* **2006**, *302*, 203–206. [[CrossRef](#)] [[PubMed](#)]
24. Zhang, B.; Luan, L.; Gao, R.; Li, F.; Li, Y.; Wu, T. Rapid and effective removal of Cr(VI) from aqueous solution using exfoliated LDH nanosheets. *Colloid Surf. A Physicochem. Eng. Asp.* **2017**, *520*, 399–408. [[CrossRef](#)]
25. Ma, L.; Islam, S.M.; Liu, H.; Zhao, J.; Sun, G.; Li, H.; Ma, S.; Kanatzidis, M.G. Selective and efficient removal of toxic oxoanions of As(III), As(V), and Cr(VI) by layered double hydroxide intercalated with MoS₄²⁻. *Chem. Mater.* **2017**, *29*, 3274–3284. [[CrossRef](#)]
26. Wang, X.; Zhu, X.; Meng, X. Preparation of a Mg/Al/Fe layered supramolecular compound and application for removal of Cr(VI) from laboratory wastewater. *RSC Adv.* **2017**, *7*, 34984–34993. [[CrossRef](#)]
27. Zhao, Y.; Li, J.G.; Fang, F.; Chu, N.; Ma, H.; Yang, X. Structure and luminescence behaviour of as-synthesized, calcined, and restored MgAlEu-LDH with high crystallinity. *Dalton Trans.* **2012**, *41*, 12175–12184. [[CrossRef](#)]
28. Smalenskaite, A.; Salak, A.N.; Ferreira, M.G.S.; Skaudzius, R.; Kareiva, A. Sol-gel synthesis and characterization of hybrid inorganic-organic Tb(III)-terephthalate containing layered double hydroxides. *Opt. Mater.* **2018**, *80*, 186–196. [[CrossRef](#)]

29. Smalenskaite, A.; Salak, A.N.; Kareiva, A. Induced neodymium luminescence in sol-gel derived layered double hydroxides. *Mendel. Commun.* **2018**, *28*, 493–494. [[CrossRef](#)]
30. Zheludkevich, M.L.; Serra, R.; Montemor, M.F.; Yasakau, K.A.; Salvado, I.M.; Ferreira, M.G.S. Nanostructured sol-gel coatings doped with cerium nitrate as pre-treatments for AA2024-T3—Corrosion protection performance. *Electrochim. Acta* **2005**, *51*, 208–217. [[CrossRef](#)]
31. To, T.X.H.; Truc, T.A.; Duong, N.T.; Vu, P.G.; Hoang, T. Preparation and characterization of nanocontainers of corrosion inhibitor based on layered double hydroxides. *Appl. Clay Sci.* **2012**, *67*, 18–25.
32. Carneiro, J.; Caetano, A.F.; Kuznetsova, A.; Maia, F.; Salak, A.N.; Tedim, J.; Scharnagl, N.; Zheludkevich, M.L.; Ferreira, M.G.S. Polyelectrolyte-modified layered double hydroxide nanocontainers as vehicles for combined inhibitors. *RSC Adv.* **2015**, *5*, 39916–39929. [[CrossRef](#)]
33. Guo, L.; Wu, W.; Zhou, Y.F.; Zhang, F.; Zeng, R.C.; Zeng, J.M. Layered double hydroxide coatings on magnesium alloys: A review. *J. Mater. Sci. Technol.* **2018**, *34*, 1455–1466. [[CrossRef](#)]
34. Richetta, M.; Varone, A.; Pizzoferrato, R. Layered double hydroxides (LDH): Applications of interest to metallurgy. *Metall. Ital.* **2019**, *2*, 5–14.
35. Sato, T.; Fujita, H.; Endo, T.; Shimada, M.; Tsunashima, A. Synthesis of hydrotalcite-like compounds and their physico-chemical properties. *React. Solids* **1988**, *5*, 219–228. [[CrossRef](#)]
36. Klemkaite, K.; Prosycevas, I.; Taraskevicius, R.; Khinsky, A.; Kareiva, A. Synthesis and characterization of layered double hydroxides with different cations (Mg, Co, Ni, Al), decomposition and reformation of mixed metal oxides to layered structures. *Centr. Eur. J. Chem.* **2011**, *9*, 275–282. [[CrossRef](#)]
37. Jitianu, M.; Zaharescu, M.; Bălăsoiu, M.; Jitianu, A. The sol-gel route in synthesis of Cr(III)-containing clays. Comparison between Mg-Cr and Ni-Cr anionic clays. *J. Sol-Gel Sci. Technol.* **2003**, *26*, 217–221. [[CrossRef](#)]
38. Othman, M.R.; Helwani, Z.; Martunus, F.W.J.N. Synthetic hydrotalcites from different routes and their application as catalysts and gas adsorbents: A review. *Appl. Organometal. Chem.* **2009**, *23*, 335–346. [[CrossRef](#)]
39. Inayat, A.; Klumpp, M.; Schwieger, W. The urea method for the direct synthesis of ZnAl layered double hydroxides with nitrate as the interlayer anion. *Appl. Clay Sci.* **2011**, *51*, 452–459. [[CrossRef](#)]
40. Naseem, S.; Gevers, B.; Boldt, R.; Labuschagn, F.J.W.J.; Leuteritz, A. Comparison of transition metal (Fe, Co, Ni, Cu, and Zn) containing tri-metal layered double hydroxides (LDHs) prepared by urea hydrolysis. *RSC Adv.* **2019**, *9*, 3030–3040. [[CrossRef](#)]
41. Kovanda, F.; Kolousek, D.; Cilova, Z.; Hulinsky, V. Crystallization of synthetic hydrotalcite under hydrothermal conditions. *Appl. Clay Sci.* **2005**, *28*, 101–109. [[CrossRef](#)]
42. Utracki, L.A.; Sepehr, M.; Boccaleri, E. Synthetic, layered nanoparticles for polymeric nanocomposites WNCO. *Polym. Adv. Technol.* **2007**, *18*, 1–37. [[CrossRef](#)]
43. Olf, H.W.; Torres-Dorante, L.O.; Eckelt, R.; Kosslick, H. Comparison of different synthesis routes for Mg-Al layered double hydroxides (LDH): Characterization of the structural phases and anion exchange properties. *Appl. Clay Sci.* **2009**, *43*, 459–464. [[CrossRef](#)]
44. Liu, J.H.; Zhang, Y.; Yu, M.; Li, S.M.; Xue, B.; Yin, X.L. Influence of embedded ZnAlCe-NO₃-layered double hydroxides on the anticorrosion properties of sol-gel coatings for aluminum alloy. *Progr. Org. Coat.* **2015**, *81*, 93–100. [[CrossRef](#)]
45. Yu, M.; Zhao, X.N.; Xiong, L.L.; Xue, B.; Kong, X.X.; Liu, J.H.; Li, S.M. Improvement of corrosion protection of coating system via inhibitor response order. *Coatings* **2018**, *8*, 365. [[CrossRef](#)]
46. Zhang, Y.S.; Wang, Y.B.; Li, C.M.; Zhou, B.T.; Cheng, K.K.; Wei, Y.Z. Preparation and corrosion resistance of the ZnAl-LDHs film on 6061 Al alloy surface. *Acta Metall. Sin.* **2018**, *54*, 1417–1427.
47. Kuang, J.; Ba, Z.X.; Li, Z.Z.; Jia, Y.Q.; Wang, Z.Z. Fabrication of a superhydrophobic Mg-Mn layered double hydroxides coating on pure magnesium and its corrosion resistance. *Surf. Coat. Technol.* **2019**, *361*, 75–82. [[CrossRef](#)]
48. Katagiri, K.; Goto, Y.; Nozawa, M.; Koumoto, K. Preparation of layered double hydroxide coating films via the aqueous solution process using binary oxide gel films as precursor. *J. Ceram. Soc. Jpn.* **2009**, *117*, 356–358. [[CrossRef](#)]
49. Kuznetsov, B.; Serdechnova, M.; Tedim, J.; Starykevich, M.; Kallip, S.; Oliveira, M.P.; Hack, T.; Nixon, S.; Ferreira, M.G.S.; Zheludkevich, M.L. Sealing of tartaric sulfuric (TSA) anodized AA2024 with nanostructured LDH layers. *RSC Adv.* **2016**, *6*, 13942–13952. [[CrossRef](#)]

50. Xue, B.; Yu, M.; Liu, J.H.; Li, S.M.; Xiong, L.L.; Kong, X.X. Synthesis of inhibitor nanocontainers with two-dimensional structure and their anticorrosion action in sol-gel coating on AA2024-T3 aluminum alloy. *J. Electrochem. Soc.* **2017**, *164*, 641–652. [[CrossRef](#)]
51. Alibakhshi, E.; Ghasemi, E.; Mahdavian, M.; Ramezanzadeh, B. Fabrication and characterization of layered double hydroxide/silane nanocomposite coatings for protection of mild steel. *J. Taiwan Inst. Chem. Eng.* **2017**, *80*, 924–934. [[CrossRef](#)]
52. Kaseem, M.; Ko, Y.G. A novel composite system composed of zirconia and LDHs film grown on plasma electrolysis coating: Toward a stable smart coating. *Ultrason. Sonochem.* **2018**, *49*, 316–324. [[CrossRef](#)] [[PubMed](#)]
53. Zhang, Y.; Yu, P.H.; Wu, J.J.; Chen, F.; Li, Y.D.; Zhang, Y.L.; Zuo, Y.; Qi, Y.A.L. Enhancement of anticorrosion protection via inhibitor-loaded ZnAlCe-LDH nanocontainers embedded in sol-gel coatings. *J. Coat. Technol. Res.* **2018**, *15*, 303–313. [[CrossRef](#)]
54. Liu, J.H.; Shi, H.B.; Yu, M.; Du, R.T.; Rong, G.; Li, S.M. Effect of divalent metal ions on durability and anticorrosion performance of layered double hydroxides on anodized 2A12 aluminum alloy. *Surf. Coat. Technol.* **2019**, *373*, 56–64. [[CrossRef](#)]
55. Sun, W.; Wu, T.T.; Wang, L.D.; Dong, C.; Liu, G.C. Controlled preparation of MgAl-layered double hydroxide/graphene hybrids and their applications for metal protection. *Ind. Eng. Chem. Res.* **2019**, *58*, 16516–16525. [[CrossRef](#)]
56. Xie, S.Y.; Wang, J.H.; Hu, W.B. Synthesis and corrosion resistance of ZnAl layered double hydroxide film on Q235 steel. *Int. J. Electrochem. Sci.* **2019**, *14*, 6773–6789. [[CrossRef](#)]
57. Wu, J.S.; Peng, D.D.; He, Y.T.; Du, X.Q.; Zhang, Z.; Zhang, B.W.; Li, X.G.; Huang, Y.Z. Hydroxide films on AA2024 and their anti-corrosive properties when combined with hybrid sol gel films. *Materials* **2017**, *10*, 426. [[CrossRef](#)]
58. Zhang, X.C.; Wang, J.X.; Zhang, C.Y.; Liu, B.; Jiang, P.; Zhao, Y.; Buhe, B.; Zhang, T.; Meng, G.Z.; Wang, F.H. Formation process of an LDHs coating on magnesium alloy by a CO₂ pressurization method. *Coatings* **2019**, *9*, 47. [[CrossRef](#)]
59. Wu, L.; Ding, X.; Zheng, Z.C.; Ma, Y.L.; Atrens, A.; Chen, X.B.; Xie, Z.H.; Sun, D.E.; Pan, F.S. Fabrication and characterization of an actively protective Mg-Al LDHs/Al₂O₃ composite coating on magnesium alloy AZ31. *Appl. Surf. Sci.* **2019**, *487*, 558–568. [[CrossRef](#)]
60. Furko, M.; Balazsi, K.; Balazsi, C. Comparative study on preparation and characterization of bioactive coatings for biomedical applications—A review on recent patents and literature. *Rev. Adv. Mater. Sci.* **2017**, *48*, 25–51.
61. Zarkov, A.; Stanulis, A.; Mikoliunaite, L.; Salak, A.N.; Kareiva, A. Organic-free synthesis of nanostructured SnO₂ thin films by chemical solution deposition. *Thin Solid Films* **2018**, *649*, 219–224. [[CrossRef](#)]
62. Conteroso, E.; Gianotti, V.; Palin, L.; Boccaleri, E.; Viterbo, D.; Milanese, M. Facile preparation methods of hydrotalcite layered materials and their structural characterization by combined techniques. *Inorg. Chim. Acta* **2018**, *470*, 36–50. [[CrossRef](#)]
63. Jonauske, V.; Stanionyte, S.; Chen, S.W.; Zarkov, A.; Juskenas, R.; Selskis, A.; Matijosius, T.; Yang, T.C.K.; Ishikawa, K.; Ramanauskas, R.; et al. Fabrication of sol-gel derived calcium hydroxyapatite coatings on patterned rough surface, characterization and assessment of its behaviour in simulated body fluid. *Coatings* **2019**, *9*, 334. [[CrossRef](#)]
64. Rubesova, K.; Havlicek, J.; Jakes, V.; Nadherny, L.; Cajzl, J.; Panek, D.; Parkman, T.; Beitlerova, A.; Kucerkova, R.; Hajek, F.; et al. Heavily Ce³⁺-doped Y₃Al₅O₁₂ thin films deposited by a polymer sol-gel method for fast scintillation detectors. *Crystengcomm* **2019**, *21*, 5115–5123. [[CrossRef](#)]
65. Vieira, D.E.L.; Sokol, D.; Smalenskaite, A.; Kareiva, A.; Ferreira, M.G.S.; Vieira, J.M.; Brett, C.M.A.; Salak, A.N. Cast iron corrosion protection with chemically modified Mg-Al layered double hydroxides synthesized using a novel approach. *Surf. Coat. Technol.* **2019**, *375*, 158–163. [[CrossRef](#)]
66. Yagami, T.; Hagiwara, M.; Fujihara, S. Fabrication of luminescence-sensing films based on surface precipitation reaction of Mg-Al-Eu LDHs. *J. Sol-Gel Sci. Technol.* **2017**, *82*, 380–389. [[CrossRef](#)]

67. Malakauskaite-Petruleviciene, M.; Stankeviciute, Z.; Niaura, G.; Prichodko, A.; Kareiva, A. Synthesis and characterization of sol–gel derived calcium hydroxyapatite thin films spin-coated on silicon substrate. *Ceram. Int.* **2015**, *141*, 7421–7428. [[CrossRef](#)]
68. Vendange, V.; Colombari, P. Determination of the hydroxyl content in gels and porous “glasses” from alkoxide hydrolysis by combined TGA and BET analysis. *J. Porous Mater.* **1996**, *3*, 193–200. [[CrossRef](#)]



© 2019 by the authors. Licensee MDPI, Basel, Switzerland. This article is an open access article distributed under the terms and conditions of the Creative Commons Attribution (CC BY) license (<http://creativecommons.org/licenses/by/4.0/>).